

International Journal of Green Energy

ISSN: 1543-5075 (Print) 1543-5083 (Online) Journal homepage: http://www.tandfonline.com/loi/ljge20

Development of an Artificial Neural Network Model for the Prediction of the Performance of a Silica-gel Desiccant Wheel

İrfan Uçkan, Tuncay Yılmaz, Ertaç Hürdoğan & Orhan Büyükalaca

To cite this article: İrfan Uçkan, Tuncay Yılmaz, Ertaç Hürdoğan & Orhan Büyükalaca (2015) Development of an Artificial Neural Network Model for the Prediction of the Performance of a Silica-gel Desiccant Wheel, International Journal of Green Energy, 12:11, 1159-1168, DOI: 10.1080/15435075.2014.895733

To link to this article: http://dx.doi.org/10.1080/15435075.2014.895733

Accepted author version posted online: 16 Apr 2014.
Published online: 16 Apr 2014.

Submit your article to this journal

Article views: 259

View related articles

View Crossmark data

Citing articles: 4 View citing articles

Full Terms & Conditions of access and use can be found at
http://www.tandfonline.com/action/journalInformation?journalCode=ljge20

Download by: [Cukurova Universitesi] **Date:** 17 August 2017, At: 05:23

International Journal of Green Energy (2015) **12**, 1159–1168
Copyright © Taylor & Francis Group, LLC
ISSN: 1543-5075 print / 1543-5083 online
DOI: 10.1080/15435075.2014.895733

Taylor & Francis
Taylor & Francis Group

Development of an Artificial Neural Network Model for the Prediction of the Performance of a Silica-gel Desiccant Wheel

İRFAN UÇKAN[1], TUNCAY YıLMAZ[2], ERTAÇ HÜRDOĞAN[3], and ORHAN BÜYÜKALACA[3]

[1]*Department of Mechanical Engineering, Yuzuncu Yil University, Van, Turkey*
[2]*Department of Mechanical Engineering, Osmaniye Korkut Ata University, Osmaniye, Turkey*
[3]*Department of Energy Systems Engineering, Osmaniye Korkut Ata University, Osmaniye, Turkey*

Downloaded by [Cukurova Universitesi] at 05:23 17 August 2017

This work presents mathematical equations derived from Artificial Neural Networks (ANNs) for the estimation of dry bulb temperature and specific humidity at the outlet of a desiccant wheel to predict useful data for designers and engineers. The neural network model comprises five inputs and two output neurons that define the outlet conditions (dry bulb temperature and specific humidity) of a desiccant wheel. The results obtained by the ANN model are compared with the actual data by using input variables. The results show that the mean absolute percentage errors for dry bulb temperature and specific humidity are found to be 0.80% and 1.56% respectively; and the correlation coefficient (R) values obtained are approximately 0.986 for both output variables. The root mean square errors, which is another significant point in this study, are found to be 0.54% and 0.18% for dry bulb temperature and specific humidity respectively.

Keywords: Desiccant wheel, Artificial neural network, Modeling, Air conditioning, Dehumidification

Introduction

A considerable part of today's energy consumption is due to the air conditioning of buildings involving both heating and cooling. Energy costs and environmental concerns obligate designers to find sustainable solutions. Desiccant cooling systems (desiccant-based air-conditioning systems) as a sustainable technology is an attractive option to investigate for that goal. Desiccant materials used in cooling systems are classified into solid (adsorbent) and liquid (absorbent), which correspond to adsorption and absorption in air dehumidification (Qiu and Riffat 2010; Yutong and Yang 2010; Li et al. 2011). Solid desiccant cooling systems using rotary desiccant wheel to dehumidify air have become increasingly popular desiccant cooling systems. In this system, the desiccant adsorbs water vapor due to the difference of water vapor pressure between the surrounding air and their surface. To make the system operate continuously, the adsorbed water vapor must be removed from the desiccant material so that it can be dried enough to adsorb water vapor in the next cycle.

Because of the importance of desiccant wheel in desiccant air-conditioning systems, many investigations have been performed on its design, modeling, and optimization (Antonellis, Joppolo, and Molinaroli 2010; Angrisani et al. 2012; Ruivo et al. 2012). With the development of computer hardware and numerical methodology, the mathematical models are being used to carry out critical investigations concerning a desiccant wheel (Zheng and Worek 1993; Gao, Mei, and Tomlinson 2005). Nia, Paassen, and Saidi (2006) presented the modeling of a desiccant wheel used for dehumidifying the ventilation air of an air-conditioning system. They used MATLAB Simulink for the simulation of the combined heat and mass transfer processes that occur in a solid desiccant wheel. They presented a heat and mass transfer model which predicts the temperature and humidity states of the outlet air from a desiccant wheel.

Artificial neural networks (ANNs) are now being increasingly recognized in the area of prediction and have been used for a wide variety of applications such as solar energy (Facao, Szabolcs, and Armando 2004; Ramedani, Omid, and Keyhani 2013), wind speed forecasting (Cadenas and Rivera 2010), and geothermal district heating system (Yabanova and Keçebaş 2013). This method is widely accepted as an alternative way to tackle complex problems. As seen in the literature research above, ANNs have been successfully applied in many fields. The advantages of ANNs are simplicity, speed, and capacity to learn from experimental data, and the other advantage is that it takes less time than experimental and numerical methods for predicting the performance of a desiccant wheel.

Şencan and Kalogirou (2005) presented a new approach using ANNs to determine the thermodynamic properties of two alternative refrigerant/absorbent couples used as working fluids in absorption heat pumps. Kalogirou (1999) presented various applications of neural networks in energy problems. Kocabas et al. (2010) modeled the effect of nozzle number and inlet pressures on the heating and cooling performance of the counter flow-type vortex tube with ANN and multi-linear regression (MLR) models by using the data obtained experimentally. Rosiek and Battles (2011) investigated solar-assisted air-conditioning system

Address correspondence to İrfan Uçkan, Department of Mechanical Engineering, Yuzuncu Yil University, 65080 Van, Turkey. E-mail: irfanuckan@yyu.edu.tr
Color versions of one or more of the figures in the article can be found online at www.tandfonline.com/ljge.

with storage tanks using ANNs. Gandhidasan and Mohandes (2011) proposed the use of an ANN-based model to simulate the relationship between the inlet and outlet parameters of a desiccant wheel. They chose lithium chloride as the liquid desiccant.

In literature, there are very few studies investigating the use of ANNs for predicting the output parameters of solid desiccant dehumidifiers.

Cejudo, Moreno, and Carrillo (2002) presented two methods for modeling the performance of a desiccant wheel. These models are a physical model, based on mass and energy balances of the process, and a neural network model, based on the training of a black box model with real data. They found that the neural network models are more adequate to simulate wheel performance. Parmar and Hindoliya (2011) developed a neural network model based on experimental observations of a desiccant wheel. Researchers used a number of training algorithms with a feed forward–back propagation method for the modeling of a desiccant wheel to identify a training algorithm with least mean square error (MSE).They found that the training algorithm trainlm (Levenberg–Marquardt training algorithm) is the most suitable one for the prediction of outputs.

In the desiccant-based air-conditioning systems, the conditions (dry bulb temperature and specific humidity) of air at the outlet of a desiccant wheel must be known to design the system. Designers generally use manufacturer's performance data given for a desiccant wheel. In this work, an ANN model has been developed for predicting the dry bulb temperature and specific humidity of air at the outlet of a silica gel desiccant wheel, and has been compared with previous researches.

Material and Method

Experimental Setup

In this study, a silica gel desiccant wheel which is a key component of desiccant air-conditioning system is used. Figure 1 gives a general view of the experimental setup, which was established in the laboratory of the Mechanical Engineering Department of Çukurova University in Adana, Turkey. The system consists of the following components: desiccant wheel, heat exchangers, direct evaporative coolers, heater, fans (used for fresh air, regeneration air, and waste air), pumps (used for direct evaporative coolers), filters, control units, and ducts.

As seen in the figure, the system has three main air channels. The first channel is used to take fresh air from outdoor and blow it into the air-conditioned room. The exhaust air is discharged from the room by means of a fan in the second channel. The third channel is used for the regeneration air stream taken from outdoors. The air flow rates are controlled by a control unit. The rotary desiccant wheel (RD) is followed by heat exchanger-1 (HE1) and heat exchanger-2 (HE2) to pre-cool the fresh air in the fresh air channel. After HE2, evaporative cooler-1 (EC1) is utilized to cool the fresh air to the blowing temperature.

The air sucked from the outdoor into the fresh air channel by a fan (process 1–2) enters RD in which moisture is absorbed by the desiccant materials of a wheel (process 2–3). The dry fresh air is pre-cooled first by the regeneration air in HE1 (process 3–4) and then enters into HE2 (process 4–5) where it is further pre-cooled by evaporatively cooled waste air. The fresh air finally enters EC1 (process 5–6), in which it is cooled down to blowing conditions and supplied to the conditioned room (state 6).

The waste air, which is sucked from conditioned room by a fan, first passes through evaporative cooler-2 (EC2) (process 7–8) and enters HE2 (process 8–9). As the waste air passes through HE2, its temperature increases and consequently the temperature of fresh air decreases. Waste air is discharged to atmosphere after HE2.

For regeneration, air is sucked from outdoor by a fan and sent into HE1. Because of heat transfer from the fresh air in HE1, temperature of the regeneration air increases (process 11–12) and that of the fresh air decreases (process 3–4). The regeneration air is sent into heat exchanger-3 (HE3) for further pre-heating (process 12–13). Electric heaters (EH) are used for heating regeneration air before entering into rotary dehumidifier (state 14).

The regeneration air is pre-heated first by recuperative HE1 and then by regenerative HE3. The heat required for the further heating of regeneration air to the desired regeneration temperature is supplied with the electric heater unit. Subsequently the regeneration air passes through the desiccant wheel (process 14–15), where its moisture content increases and then it is sent into HE3 (process 15–16). Finally, the regeneration air is discharged to the atmosphere (state 17).

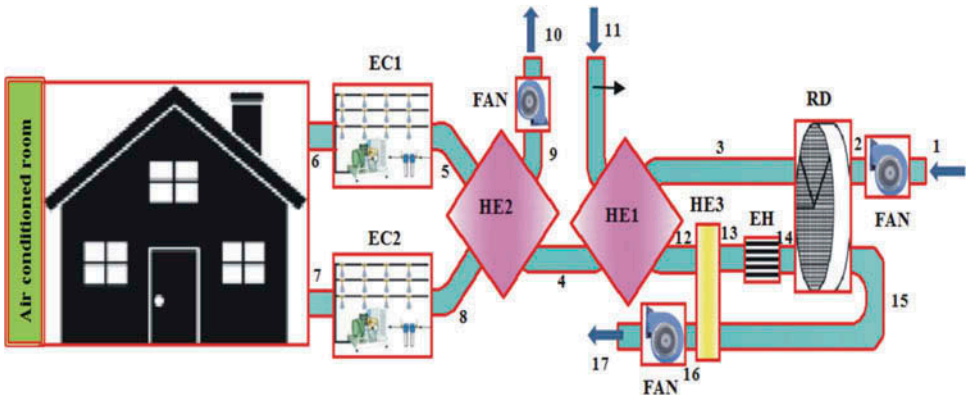


Fig. 1. General view of desiccant air-conditioning system.

Downloaded by [Cukurova Universitesi] at 05:23 17 August 2017

Downloaded by [Cukurova Universitesi] at 05:23 17 August 2017

Figure 2 illustrates an example of variation of dry bulb temperature measured with time at states 2, 3, 14, and 15 in the fresh and regeneration air channels at the inlet and outlet of a desiccant wheel. As seen in this figure, the fresh air flows through the RD and its temperature (T_3) increases up to 56°C. The RD removes moisture from the fresh air, which releases heat and increases the temperature of fresh air. Then the fresh air passes through HE1 and HE2 in which pre-cooling processes occur by the regeneration air taken from outdoor and by waste air sucked from the air-conditioned room. At the beginning of the experiment, the regeneration temperature (temperature of air at the inlet of the dehumidifier T_{14}) is set to 90°C. As can be seen in Figure 2, T_{14} increases up to a set value in a short time and stays constant at this level during the day, and the regeneration air leaves RD approximately at 50°C (T_{15}).

Figure 3 shows variation of specific humidity with time at states 1, 3, 14, and 15 in the fresh air channel and regeneration air channel at the inlet and outlet of a desiccant wheel. The fresh air and regeneration air taken from outdoor have the same specific humidity at the inlet of the system. Specific humidity of the outdoor air (W_1) varies between 15 g kg^{-1} and 16 g kg^{-1}. It decreases to 9 g kg^{-1} (W_3) after the dehumidification process (state 3) and the system has a minimum value at this state. The specific humidity of the regeneration air stream at the exit of RD (W_{15}) increases up to approximately 22 g kg^{-1} and the system has a maximum value at this state.

Figure 4 shows schematic view of a desiccant wheel used in this study. In the figure, the subscripts correspond to the state points of the system. The physical properties of a desiccant wheel are shown in Table 1. The shell and desiccant wheel are connected with a rubber pad to minimize leakage. A driving subsystem is used to rotate the desiccant wheel. It consists of an electromotor, a wheel disk, and a belt. The wheel disk and belt are used to transfer power from the electromotor to the desiccant wheel.

In the present study, the experiments are carried out instantly by measuring temperatures, flow rates, and pressure by using appropriate instruments explained below.

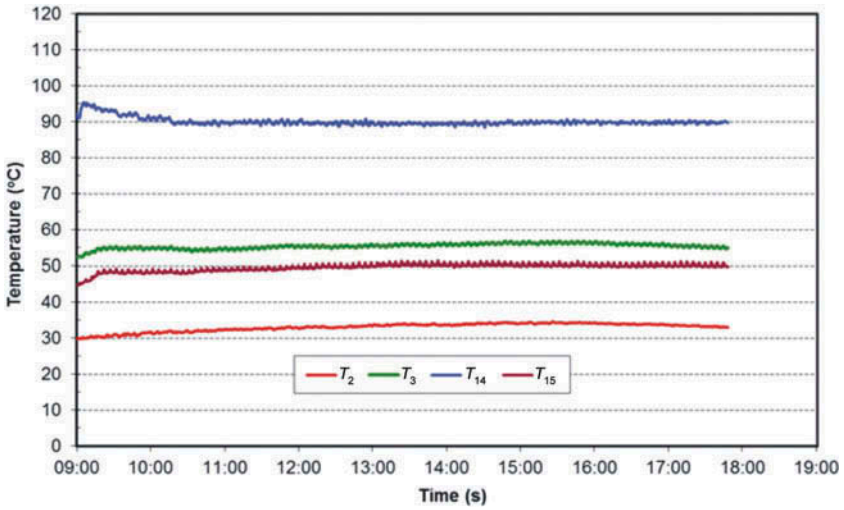


Fig. 2. Variation of dry bulb temperature with time at states 2, 3, 14, and 15.

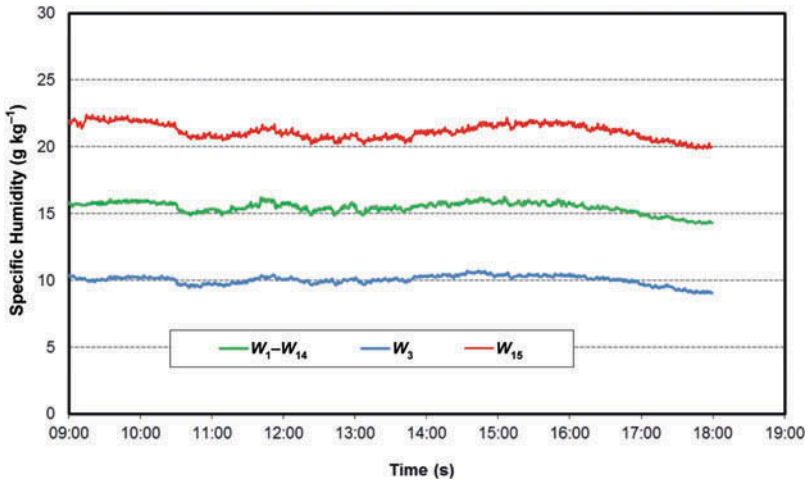


Fig. 3. Variation of specific humidity with time at states 1, 3, 14, and 15.

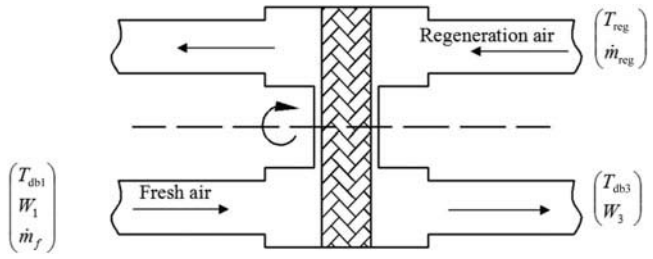


Fig. 4. Schematic view of a desiccant wheel.

Table 1. Physical Properties of a Desiccant Wheel

Properties	Description
Desiccant	Silica gel
Desiccant wheel depth	200 mm
Diameter	965 mm
Rotational speed of wheel	12 rev h^{-1}

1. Flow rates of fresh, waste, and regeneration air streams are measured using averaging (blade type) pitot tubes and differential pressure transmitters with an accuracy of ±1%.
2. Dry bulb temperature of air is measured using K-type thermocouples with an accuracy of 0.1°C.
3. Relative humidity of air is measured using relative humidity transmitters with an accuracy of ±2%.
4. Electrical signal outputs of thermocouples and transmitters are monitored and recorded with a computer-controlled data acquisition system.

Uncertainty Analysis

Uncertainty analysis is the procedure employed to assess uncertainty in a calculated result from measured variables with known values of uncertainties. For the calculation of uncertainty, the root of sum squares is used in this study (Holman 1989), which can be expressed as follows:

$$w_R = \left[\left(\frac{\partial R}{\partial x_1} w_1 \right)^2 + \left(\frac{\partial R}{\partial x_2} w_2 \right)^2 + \ldots\ldots\ldots + \left(\frac{\partial R}{\partial x_n} w_n \right)^2 \right]^{1/2}, \tag{1}$$

where the result R is a given function of independent variables, $x_1, x_2, \ldots x_n$, and $w_1, w_2, \ldots w_n$ are the uncertainties in independent variables.

Equation (1) is a general equation used to calculate uncertainty in each result. Temperature, relative humidity, and mass flow rate are measured with appropriate instruments. The total uncertainties of the measurements are estimated to be ±0.3°C for air temperature, ±2.51% for relative humidity, and ±2.89% for mass flow rate.

Artificial Neural Networks

Artificial neural networks are non-linear mapping structures based on the human brain functioning. These are powerful tools for modeling, especially when the underlying data relationship is unknown. ANNs can identify and learn correlated patterns between input and output data sets. Instead of complex rules and mathematical routines, ANNs are able to learn key information patterns within a multi-information domain. The most widely used learning algorithm in ANNs is the Back Propagation Algorithm.

In order to suit the consistency of the model, the values applied in the input and output layers are normalized by the following formula in the range of 0.1–0.9, and then returned to the original values after simulation (Bilgili, Sahin, and Sangun 2013):

$$X_N = 0.8 \left(\frac{X_r - X_{\min}}{X_{\max} - X_{\min}} \right) + 0.1, \tag{2}$$

where X_N, X_r, $X_{\min}$, and $X_{\max}$ are the normalized, real, minimum, and maximum values respectively.

To calculate the neuron j mathematically, the following equations may be described (Haykin 1994):

$$u_j = \sum_{i=1}^{p} w_{ji} x_i, \tag{3}$$

and

$$y_j = \varphi(u_j - \theta_j), \tag{4}$$

where u_j is the summation function, w_{ji} is the weight of the connection neuron (i) to neuron (j), x_i is the input signal, θ_j is the threshold, which is an external parameter of neuron (j), and y_j is the output signal of the neuron (j).

In the present study, the Levenberg–Marquardt training algorithm is used to evaluate the wheel. As the most common form of activation function, logistic sigmoid (logsig) and linear transfer functions are used in the construction of ANNs. These functions have been used for hidden and output layers of networks as an activation function respectively.

The activation function used is given by:

$$F(y_j) = \frac{1}{1 + e^{-y_j}} \tag{5}$$

The computer program is performed using MATLAB software (Math Works 2009). The performance of the model is assessed on the basis of three characteristics: the mean absolute error (MAE), the mean absolute percentage error (MAPE), and the root mean square error (RMSE) (Bilgili and Sahin 2010).

These are given as follows:

$$\text{MAE} = \frac{1}{n} \sum_{i=1}^{n} |a_i - p_i|, \tag{6}$$

$$\text{MAPE} = \frac{1}{n} \sum_{i=1}^{n} \frac{|a_i - p_i|}{a_i} \times 100, \tag{7}$$

Downloaded by [Cukurova Universitesi] at 05:23 17 August 2017

$$\text{RMSE} = \sqrt{\frac{1}{n}\sum_{i=1}^{n}(a_i - p_i)^2}, \tag{8}$$

where a is the actual value, p is the predicted value, and n is the total number of value.

The ANN architecture of the model is shown in Figure 5. As seen in this figure, the network architecture has one hidden layer with eight neurons. For a set of training procedures, the minimum error is found with only one hidden layer for eight neurons. Five neurons are used as input signals in the input layer and two neurons are utilized in the output layer of the network. As input signals, the architecture consists of the outdoor air dry bulb temperature (T_{db1}), the outdoor air specific humidity (W_1), which is calculated using the relative humidity and dry bulb temperature measured on the system, the regeneration temperature (T_{reg}), the fresh air mass flow rate ($\dot{m}_f$), and the regeneration air mass flow rate ($\dot{m}_{\text{reg}}$). After rotary desiccant wheel, there are two parameters to be estimated, namely: dry bulb temperature (T_{db3}) and specific humidity (W_3). The range values of input and output variables are given in Table 2.

The model used in this study is based on a feed forward BP network. Normally a BP has an input and output layer and a certain number of hidden layers. The input and output layers are necessary, the number of hidden layers is free but generally a single layer is chosen. In the present work, the selected network consists of one input layer, one output layer, and one hidden layer for processing the data.

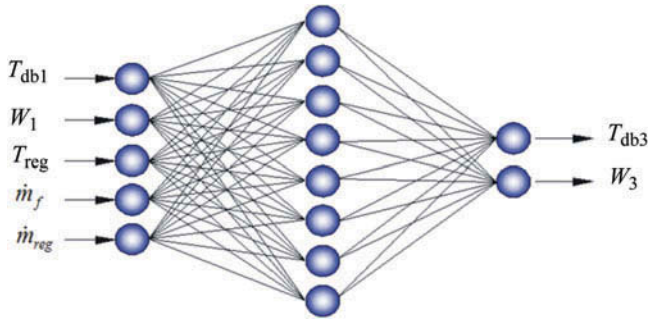


Fig. 5. The artificial neural network architecture of the model.

Table 2. Operating Parameters and Their Ranges Used for Generating Data

	Unit	Min.	Max.
Input of a desiccant wheel			
Air inlet dry bulb temperature (T_{db1})	°C	27	35
Air inlet specific humidity (W_1)	g kg^{-1}	9.57	18.16
Regeneration temperature (T_{reg})	°C	90	110
Fresh air mass flow rate ($\dot{m}_f$)	kg s^{-1}	0.59	1.27
Regeneration air mass flow rate ($\dot{m}_{\text{reg}}$)	kg s^{-1}	0.51	1.34
Output of a desiccant wheel			
Air outlet dry bulb temperature (T_{db3})	°C	53	73
Air outlet specific humidity (W_3)	g kg^{-1}	4.76	11.51

Results and Discussion

Various experiments have been carried out in the cooling season of 2011. The temperature of regeneration air has been adjusted to 90°C, 100°C, and 110°C. The measurements have been taken between 900 and 1800 hours.

Artificial neural networks rely on trial and error and other factors such as network structure, amount of training data, amount of testing data, training function, learning function, and performance function (Mohammad et al. 2013).

In this work, the data set for every operating parameter included 19,832 patterns that are obtained from the data acquisition system. To further improve model's accuracy, a large amount of data is used. ANNs have a two-step procedure; these are named training and testing procedures. First of all, the training procedure is applied to design the model, and then the testing procedure is applied to evaluate the performance of the network. The ratio of training and testing procedure is 70% and 30% respectively. During the first stage of the experimental data analysis, a sample of 13,882 patterns has been considered for training the neural network and the remaining 5949 patterns are selected and used as the test data set. When network training is successfully completed, the network is tested on a reliable set of experimental data.

The new formulations that depend on the input parameters of a desiccant wheel are given in Eqs. (9)–(12). According to these equations, the dry bulb temperature and the specific humidity of air at the outlet of a desiccant wheel can be predicted. The mathematical formulations derived from the ANN model are presented. The equations that can be used for the prediction of the dry bulb temperature and specific humidity are expressed as follows:

$$T_{\text{db3}}7 = -0.0380F_1 + 2.0336F_2 - 0.0797F_3 - 0.0447F_4 - 0.1842F_5 + 0.2375F_6 - 0.2546F_7 + 0.0979F_8 - 0.3914, \tag{9}$$

$$W_3 = -0.1048F_1 + 0.2098F_2 - 0.2807F_3 - 0.0638F_4 + 1.4085F_5 - 0.0425F_6 - 0.0621F_7 + 0.1023F_8 - 0.0782. \tag{10}$$

Here, F_i ($i = 1,\ 2 \ldots 8$) can be calculated by the sigmoid function according to Eq. (11),

$$F_i = \frac{1}{1 + e^{-E_i}}. \tag{11}$$

The summation function of neuron (i) is calculated by Eq. (12), where input values are written directly for an easy understanding of the equation,

$$E_i = w_{1i}T_{\text{db1}} + w_{2i}W_1 + w_{3i}T_{\text{reg}} + w_{4i}\dot{m}_f + w_{5i}\dot{m}_{\text{reg}} + \theta_i. \tag{12}$$

In Eq. (12), the first five values are the multiplication of input parameters with their weights given in Table 3 for the ith neuron and the last constant value represents the bias term. Thus, the terms of E_1 to E_8 and F_1 to F_8 represent the summation and activation functions of each neuron of the hidden layer respectively.

Downloaded by [Cukurova Universitesi] at 05:23 17 August 2017

Table 3. Weights and Bias of Each Neuron

i	$w_{1(i)}$	$w_{2(i)}$	$w_{3(i)}$	$w_{4(i)}$	$w_{5(i)}$	θ_i
1	6.9669	12.9163	6.5484	−0.5042	−16.3589	−16.1225
2	0.4660	0.7696	1.1283	0.3930	−0.5336	−1.4542
3	−1.4854	−2.9248	7.0039	2.0965	−7.7519	2.2443
4	0.0831	11.9687	15.5063	−22.1349	20.6996	−12.1353
5	0.1915	3.0084	0.0385	0.1524	0.3292	−2.5781
6	−1.5579	−0.4170	−11.9010	−20.7800	−8.9601	16.0559
7	2.2769	−0.7137	15.7209	18.3041	−1.0372	−24.0467
8	−2.1632	−7.9888	18.5907	−8.5778	−14.2038	9.7575

The results obtained from the training and the testing of the model is fairly good in both the cases. For the testing data sets, scatter diagrams of the ANN prediction against the actual values are drawn to indicate the performances of the model. Figures 6 and 7 present the comparison between the predicted and actual (experimental) dry bulb temperatures and the specific humidity of air at the outlet of a desiccant wheel for different regeneration temperatures respectively. Figure 6 indicates that the difference between the predicted and the measured dry bulb temperatures varies by about 0.2–0.8°C. Figure 7 depicts that the difference between the predicted and the measured specific humidity varies approximately by 0.03–0.2 g kg^{-1}.

As seen in these figures, the results of prediction have a very close agreement with the corresponding actual measurements. These figures also show that ANNs are able to predict dry bulb temperature and specific humidity at the outlet of a silica gel desiccant wheel reasonably well.

The performance values, such as MAE, MAPE, and RMSE, for the training and testing procedures are given for the training and testing test data in Table 4.

The values of statistical indicators have been obtained by taking the average of the values. The MAE values of dry bulb temperature differ from the actual values, and these values are 0.37°C and 0.47°C for the testing and training data set respectively. As seen in Table 4, the MAE for dry bulb temperature in the training data set is lower than that of the testing data set. It is seen in Table 4 that the dry bulb temperature has a minimum percentage error of 0.60% in the whole training and testing data set, but the specific humidity has a maximum percentage error of 1.60%. In addition, the maximum and minimum correlation coefficients (R) between the actual and predicted values for dry bulb temperature are found to be 0.9954 and 0.9860 in the training and testing data set respectively. Another significant point in this study is the RMSE used to compare the closeness of the modeled values with the actual values. The RMSE is found to be much lower for the specific humidity and the dry bulb temperature. In the testing data set, RMSE is found to be 0.54% and 0.18% for the dry bulb temperature and the specific humidity respectively. As seen in this table, the performance values of the training procedure are in general better than the performance values of the testing procedure.

Figure 8 shows the performance of the training data set of dry bulb temperature at the outlet of a desiccant wheel with $R^2 = 0.9908$. Figure 9 shows the performance of the training data set of specific humidity at the outlet of a desiccant wheel with $R^2 = 0.9859$. The maximum percentage difference values between the measured and predicted dry bulb temperature and specific humidity at the outlet of a silica gel desiccant wheel are 3.2% and 7.8% respectively. Therefore, the predicted results of the neural network comply with the experimental data. As depicted in Figures 8 and 9, predicted dry bulb temperature and specific humidity values present very good agreement with the experimentally measured values.

Only a small number of research papers have investigated the use of ANNs for predicting the output parameters of solid desiccant dehumidifiers. Considering the performance of the training data set, in Table 5 R^2 is compared between the proposed ANN model and the data from Koronaki, Rogdakis, and Kakatsiou (2012).

As seen in Table 5, the output parameters show that the current study provides a reasonable degree of accuracy according to Koronaki, Rogdakis, and Kakatsiou (2012) for dry bulb temperatures ($R^2 = 0.9908$) and the specific humidity ($R^2 = 0.9859$) of air at the outlet of a desiccant wheel.

Considering the whole set of measurements, it is compared between the proposed ANN model and the other correlation models for desiccant wheels from literature. Several research papers have been dedicated to explore the issues on temperature and specific humidity of air at the outlet of a desiccant wheel. Stabat and Marchio (2008) developed a desiccant wheel behavioral model. A study of error propagation in a desiccant evaporative cooling system shows that the errors for the desiccant wheel outlet temperature and specific humidity are ±2°C and ±1 g kg^{-1} respectively. Panaras et al. (2010) present an experimental validation of a simplified approach for a desiccant wheel model based on the concept of the analogy method and the formulation proposed by Jurinak (1982) for respective combined potentials. They calculated the RMSE of temperature and the specific humidity of air at the outlet of a desiccant wheel and found these to be 1.24°C and 0.30 g kg^{-1} respectively.

It is observed in this work that the results found for the temperature and specific humidity of air at the outlet of a desiccant wheel are better than those found in former studies.

Errors obtained in this model are within acceptable limits. It can be concluded that the ANN technique can successfully predict dry bulb temperature and specific humidity at the outlet of a desiccant wheel.

Downloaded by [Cukurova Universitesi] at 05:23 17 August 2017

Downloaded by [Cukurova Universitesi] at 05:23 17 August 2017

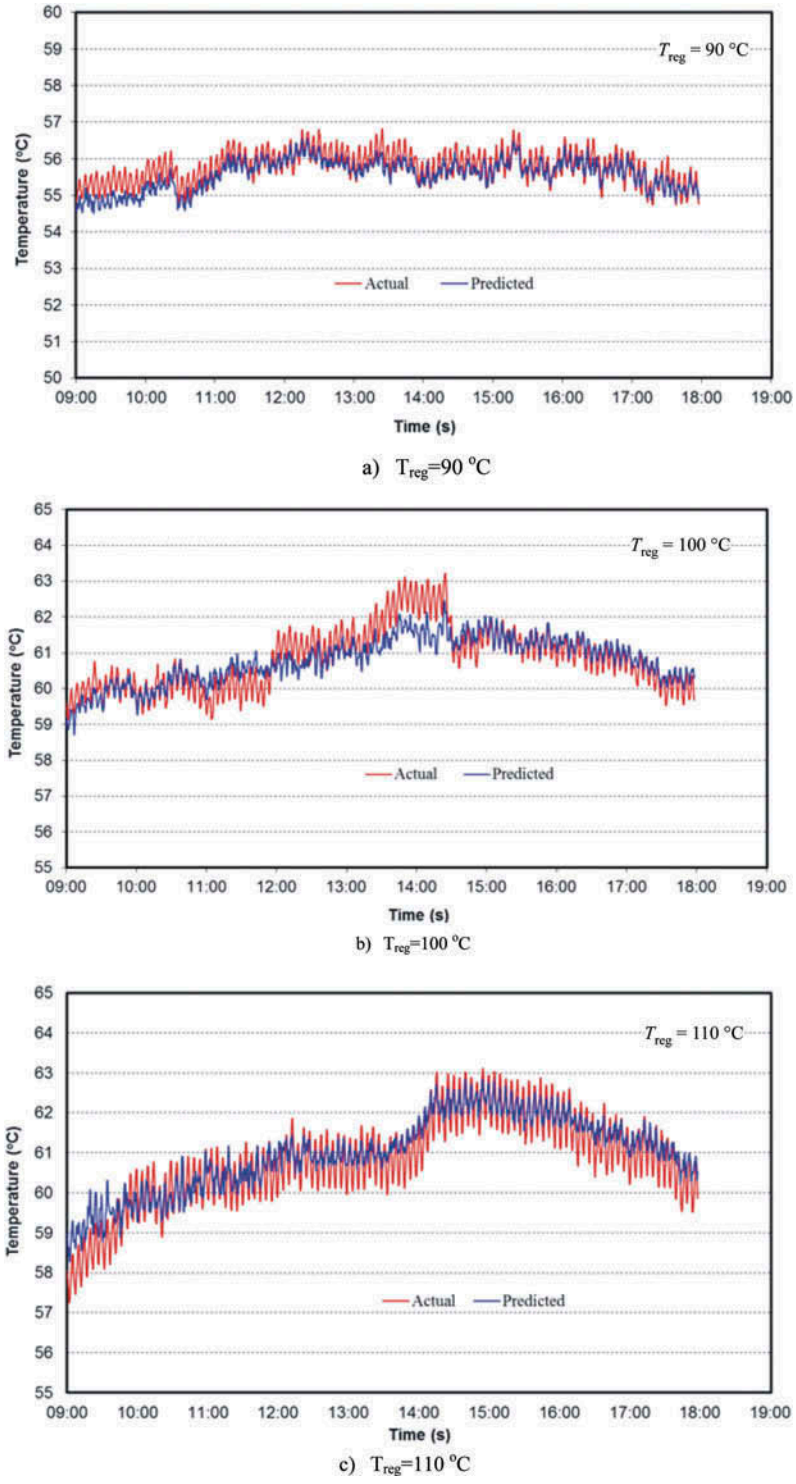


Fig. 6. Comparison between ANN model and the actual results of the outlet dry bulb temperature T_{db3} for different regeneration temperatures during the day.

Conclusions

The objective of this work was to develop a model that could be used to predict dry bulb temperature and specific humidity of air at the outlet of a desiccant wheel. For this purpose, an ANN model was used, which was successfully applied to a desiccant wheel used in a desiccant air-conditioning system. The following conclusions may be derived:

1. In the analysis of a desiccant air-conditioning system, the temperature and specific humidity of air at the outlet of a desiccant wheel must be known. In this case, we need to find

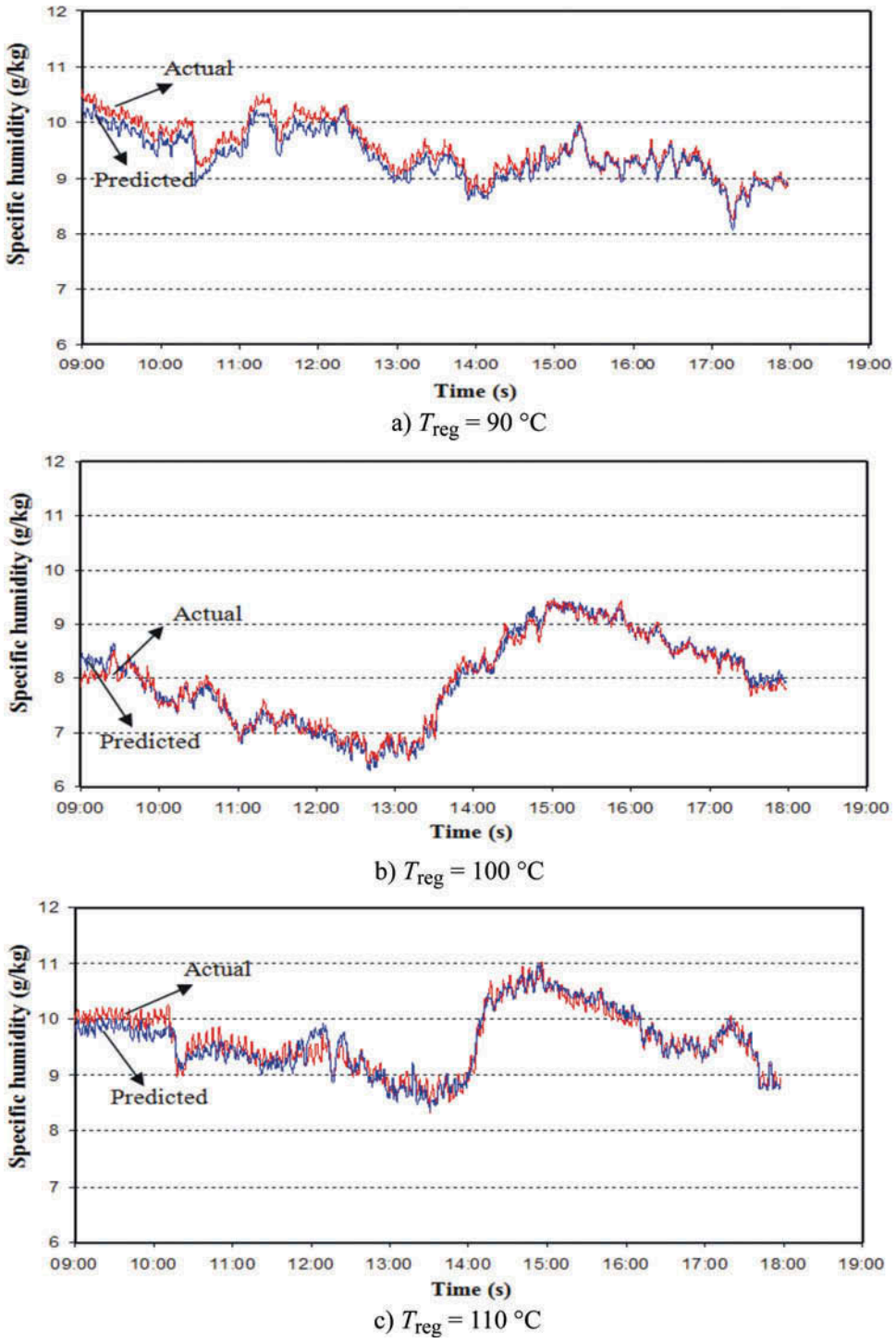


Fig. 7. Comparison between ANN model and the actual results of specific outlet humidity W_3 for different regeneration temperatures during the day.

the manufacturer's performance curve of a desiccant wheel. However, this paper presents mathematical equations derived from ANNs for the estimation of dry bulb temperature and the specific humidity at the outlet of a desiccant wheel.

2. Mean absolute error and RMSE are found to be 0.47°C and 0.54°C for the dry bulb temperature and 0.14 and 0.18 g kg^{-1} for specific humidity in the testing data respectively. It is observed that the mean absolute percentage errors in the whole testing and training data set are less than 2% for the output values of a desiccant wheel.
3. It is observed that the predicted values obtained using this model are very close to the experimental values, and the errors are within the acceptable limits.

Downloaded by [Cukurova Universitesi] at 05:23 17 August 2017

Table 4. Performance Values of the Model

	Training data set				*Testing data set*			
Output	MAE	MAPE	RMSE	R	MAE	MAPE	RMSE	R
T_{db}	0.37	0.60	0.49	0.9954	0.47	0.80	0.54	0.9860
W	0.127	1.60	0.16	0.9929	0.140	1.56	0.18	0.9865

Table 5. Comparison of Present Study With Literature

References	Desiccant wheel	Input parameters	Output parameters	Network structure applied	R^2
Present study	Silica gel	Inlet dry bulb temperature of process air	Outlet dry bulb temperature of process air	Single hidden layer	0.9908
		Inlet specific humidity of process air	Outlet specific humidity of process air		0.9859
		Inlet dry bulb temperature of regeneration air			
		Mass flow rate of process air			
		Mass flow rate of regeneration air			
Koronaki, Rogdakis, and Kakatsiou (2012)	Silica gel	Inlet dry bulb temperature of process air	Outlet dry bulb temperature of process air	Single hidden layer	0.984
		Inlet specific humidity of process air	Outlet specific humidity of process air		0.778
		Inlet dry bulb temperature of regeneration air	Outlet dry bulb temperature of regeneration air		0.987
		Inlet specific humidity of regeneration air	Outlet specific humidity of regeneration air		0.789

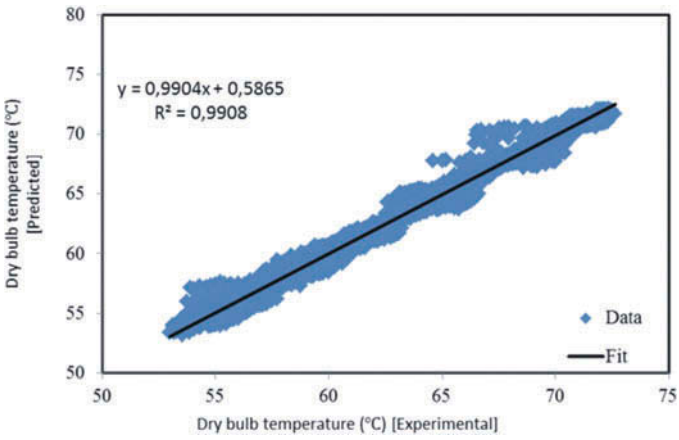


Fig. 8. Prediction of neural network model for dry bulb temperature at the outlet of a desiccant wheel.

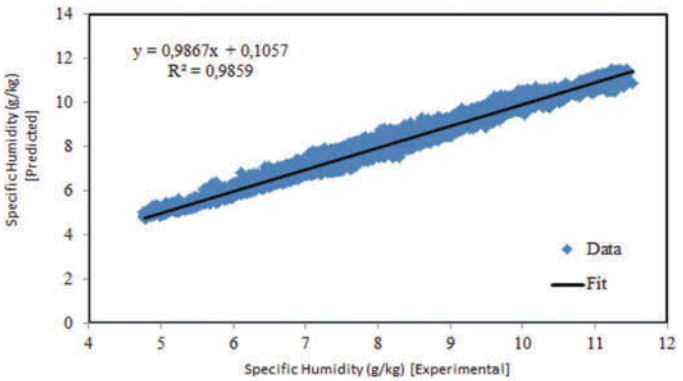


Fig. 9. Prediction of neural network model for specific humidity at the outlet of a desiccant wheel.

4. In this study, a new method of calculation of dry bulb temperature and specific humidity at the outlet of a desiccant wheel is proposed to predict useful data for designers.

Nomenclature

a_i	Actual value
E_i	Summation function
F_i	Sigmoid function
$\dot{m}$	Mass flow rate (kg s^{-1})
MAE	Mean absolute error (%)
MAPE	Mean absolute percentage error (%)
N	The total number of value
p_i	Predicted value
RMSE	Root mean square error (%)
T	Temperature (°C)
W	Specific humidity (g kg^{-1})
w_{ji}	Weight of the connection from input i to neuron j
x_i	Input signal

Downloaded by [Cukurova Universitesi] at 05:23 17 August 2017

Greek letters

θ_j	Bias of the neuron j

Subscripts

1, 2 . . . 17	State numbers
db	Dry bulb
F	Fresh air
I	Inlet air
Min	Minimum
Max	Maximum
N	Normalize
reg	Regeneration air

References

Angrisani, G., F. Minichiello, C. Roselli, and M. Sasso. 2012. Experimental analysis on the dehumidification and thermal performance of a desiccant wheel. *Applied Energy* 90:563–72.

Antonellis, S.D., C.M. Joppolo, and L. Molinaroli. 2010. Simulation, performance analysis and optimization of desiccant wheels. *Energy and Buildings* 42:1386–93.

Cadenas E., and Rivera W. 2010. Wind speed forecasting in three different regions of Mexico, using a hybrid ARIMA and ANN model. *Renewable Energy* 35:2732–38.

Bilgili, M., B. Sahin, and L. Sangun. 2013. Estimating soil temperature using neighboring station data via multi-nonlinear regression and artificial neural network models. *Enviromental Monitoring and Assesment* 185:347–58.

Bilgili, M., and B. Sahin. 2010. Comparative analysis of regression and artificial neural network models for wind speed prediction. *Meteorological Atmospheric Physics* 109:61–72.

Cejudo, J.M., R. Moreno, and A. Carrillo. 2002. Physical and neural network models of a silica gel desiccant wheel. *Energy and Buildings* 34:837–44.

Facao J., V. Szabolcs, and C.O. Armando.2004. Evaluation of the use of artificial neural networks for the simulation of hybrid solar collectors. *International Journal of Green Energy* 1:337–52.

Gandhidasan, P., and M.A. Mohandes. 2011. Artificial neural network analysis of liquid desiccant dehumidification system. *Energy* 36:1180–86.

Gao, Z., V.C. Mei, and J.J. Tomlinson. 2005. Theoretical analysis of dehumidification process in a desiccant wheel. *Heat Mass Transfer* 41:1033–42.

Haykin, S. 1994. *Neural networks, a comprehensive foundation*. New Jersey: Prentice-Hall.

Holman, J.P. 1989. *Experimental methods for engineers*, 5th ed. New York, NY: McGraw Hill.

Jurinak, J.J. 1982. Open cycle solid desiccant cooling-component models and system simulations. PhD Thesis, Univ. of Wisconsin-Madison, Madison, WI.

Kalogirou, S.A. 1999. Applications of artificial neural networks in energy systems: a review. *Energy Conversion and Management* 40:1073–87.

Kocabas, F., M. Korkmaz, U. Sorgucu, and S. Donmez. 2010. Modeling of heating and cooling performance of counter flow type vortex tube by using artificial neural network. *International Journal of Refrigeration* 33:963–72.

Koronaki, I.P., E. Rogdakis, and T. Kakatsiou. 2012. Thermodynamic analysis of an open cycle solid desiccant cooling system using artificial neural network. *Energy Conversion and Management* 60: 152–60.

Li H., Y.J. Dai, Y. Li, D. La, and R.Z. Wang. 2011. Experimental investigation on a one-rotor two-stage desiccant cooling/heating system driven by solar air collectors. *Applied Thermal Engineering* 31: 3677–83.

Math Works. 2009. *Matlab, version 7 (R2009b)*. Natick, MA: The Math Works.

Mohammad, A., S. Mat, M.Y Sulaiman, K. Sopian, and A. Abduljalil. 2013. Implementation and validation of an artificial neural network for predicting the performance of a liquid desiccant dehumidifier. *Energy Conversion and Management* 67:240–50.

Nia, F.E., D.V. Paassen, and M.H. Saidi. 2006. Modeling and simulation of desiccant wheel for air conditioning. *Energy and Buildings* 38:1230–9.

Parmar, H., and D.A. Hindoliya. 2011. Artificial neural network-based modelling of desiccant wheel. *Energy and Buildings* 43: 3505–13.

Panaras, P., E. Mathioulakisa, V. Belessiotis, and N. Kyriakisb. 2010. Experimental validation of a simplified approach for a desiccant wheel model. *Energy and Buildings* 42:1719–25.

Qiu, G.Q., and S.B. Riffat. 2010. Experimental investigation of a novel air dehumidifier using liquid desiccant. *International Journal of Green Energy* 7:174–80.

Ramedani Z., M. Omid, and A. Keyhani. 2013. Modeling solar energy potential in a Tehran province using artificıal neural networks. *International Journal of Green Energy* 10:427–41.

Rosiek, S., and F.J. Batlles. 2011. Performance study of solar-assisted air-conditioning system provided with storage tanks using artificial neural networks. *International Journal of Refrigeration* 34:1446–54.

Ruivo, C.R., A. Andrés, J.J. Costa, and F. Domínguez. 2012. A new approach to the effectiveness method for the simulation of desiccant wheels with variable inlet states and airflows rates. *Applied Thermal Engineering* 58:1–9.

Şencan, A., and S.A. Kalogirou. 2005. A new approach using artificial neural networks for determination of the thermodynamic properties of fluid couples. *Energy Conversion and Management* 46:2405–18.

Stabat, P., and D. Marchio. 2008. Heat-and-mass transfers modeled for rotary desiccant dehumidifiers. *Applied Energy* 85: 128–42.

Yabanova I., and Keçebaş A. 2013. Development of ANN model for geothermal district heating system and a novel PID-based control strategy. *Applied Thermal Engineering* 51:908–16.

Yutong, L., and Y. Hongxing. 2010. Experimental study of an open-cycle solar collector/regenerator using liquid desiccant for air conditioning. *International Journal of Green Energy* 7:273–88.

Zheng, W., and M. Worek. 1993. A numerical simulation of combined heat and mass transfer processes in a rotary dehumidifier. *Numerical Heat Transfer* 23:211–32.

Downloaded by [Cukurova Universitesi] at 05:23 17 August 2017